Energetic and Mechanistic Studies of Glucoamylase Using Molecular Recognition of Maltose OH Groups Coupled with Site-Directed Mutagenesis

Michael R. Sierks*,‡ and Birte Svensson*,§

Department of Chemical and Biochemical Engineering, 1000 Hilltop Circle, University of Maryland Baltimore County, Baltimore, Maryland 21250, and Department of Chemistry, Carlsberg Laboratory, Gamle Carlsberg Vej 10, DK-2500 Copenhagen, Valby, Denmark

Received November 1, 1999; Revised Manuscript Received March 31, 2000

ABSTRACT: Molecular recognition using a series of deoxygenated maltose analogues was used to determine the substrate transition-state binding energy profiles of 10 single-residue mutants at the active site of glucoamylase from *Aspergillus niger*. The individual contribution of each substrate hydroxyl group to transition-state stabilization with the wild type and each mutant GA was determined from the relation $\Delta(\Delta G^{\ddagger}) = -RT \ln[(k_{cat}/K_M)_x/(k_{cat}/K_M)_y]$, where x represents either a mutant enzyme or substrate analogue and y the wild-type enzyme or parent substrate. The resulting binding energy profiles indicate that disrupting an active site hydrogen bond between enzyme and substrate, as identified in crystal structures, not only sharply reduces or eliminates the energy contributed from that particular hydrogen bond but also perturbs binding contributions from other substrate hydroxyl groups. Replacing the active site acidic groups, Asp55, Glu180, or Asp309, with the corresponding amides, and the neutral Trp178 with the basic Arg, all substantially reduced the binding energy contribution of the 4′- and 6′-OH groups of maltose at subsite −1, even though both Glu180 and Asp309 are localized at subsite 1. In contrast, the substitution, Asp176 → Asn, located near subsites −1 and 1, did not substantially perturb any of the individual hydroxyl group binding energies. Similarly, the substitutions Tyr116 → Ala, Ser119 → Tyr, or Trp120 → Phe also did not substantially alter the energy profiles even though Trp120 has a critical role in directing conformational changes necessary for activity. Since the mutations at Trp120 and Asp176 reduced k_{cat} values by 50- and 12-fold, respectively, a large effect on k_{cat} is not necessarily accompanied by changes in hydroxyl group binding energy contributions. Two substitutions, Asn182 → Ala and Tyr306 → Phe, had significant though small effects on interactions with 3- and 4′-OH, respectively. Binding interactions between the enzyme and the glucosyl group in subsite −1, particularly with the 4′- and 6′-OH groups, play an important role in substrate binding, while subsite 1 interactions may play a more important role in product release.

Glucoamylase (GA,[1] 1,4-α-D-glucan glucohydrolase, EC 3.2.1.3) is an exohydrolase that catalyzes the release of D-glucose from the nonreducing ends of starch and related oligo- and polysaccharides with inversion of the anomeric configuration (*1*). GA hydrolyzes both α-1,4- and α-1,6-glucosidic linkages at a single active site (*2*), with an approximately 500-fold higher activity (determined by k_{cat}/K_M) for the α-1,4-linkage (*3*).

The active site of GA contains a general acid catalyst, Glu179 of *Aspergillus awamori* GA, that donates a proton to the oxygen of the scissile glucosidic bond and a catalytic base, Glu400, promoting the nucleophilic attack of a water molecule on C-1 of the glycon moiety in the substrate transition-state oxocarbenium ion (*4*−*9*). Comparison of the primary structures of 15 yeast and fungal GAs indicates six highly conserved stretches (*10*−*12*) located at the six different α → α segments connecting secondary structural elements in the catalytic $(\alpha/\alpha)_6$-barrel domain of GA. These six segments form a major part of the active site pocket (*5*, *7*, *9*, *13*) which is postulated to contain seven subsites, each of which binds a glucosyl residue of the substrate (*1*, *14*, *15*). The hydrolytic site is located between subsite −1, the terminal subsite, and subsite 1 (Figure 1). The affinities of these subsites for a glucosyl moiety previously were thought to be dominated by a very large affinity at subsite 1, with a small positive or negative affinity at subsite −1 (*1*, *14*−*17*). Pre-steady-state kinetic analysis, however, suggested the more important role for subsite −1 (*18*, *19*). Subsite affinities estimated from pre-steady-state association constants provide an affinity map very different from that obtained using steady-state parameters, indicating that initial binding is controlled by a high affinity at subsite −1, and that subsite 1 has a much lower affinity (*20*).

GA active site interactions between side chains and various oligosaccharide inhibitors have been identified crystallographically (*5*−*7*, *9*, *13*), and site-directed mutagenesis studies either predicted or confirmed many of these critical interactions, particularly in subsites −1 and 1 (*3*, *4*, *8*, *21*, *22*). Moreover, molecular recognition of either maltose or isomaltose analogues identified key functional OH groups

* To whom correspondence should be addressed. M.R.S.: Department of Chemical and Biochemical Engineering, 1000 Hilltop Circle, University of Maryland Baltimore County, Baltimore, MD 21250; telephone, (410) 455-3403; fax, (410) 455-1049; e-mail, sierks@umbc.edu. B.S.: Department of Chemistry, Carlsberg Laboratory, Gamle Carlsberg Vej 10, DK-2500 Copenhagen, Valby, Denmark; telephone, 45 33275345; fax, 45 33274708; e-mail, bis@crc.dk.

‡ University of Maryland Baltimore County.

§ Carlsberg Laboratory.

[1] Abbreviation: GA, glucoamylase.

10.1021/bi9925219 CCC: $19.00
Published on Web 06/27/2000

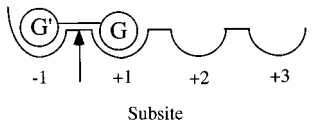

FIGURE 1: Schematic of maltose bound to the glucoamylase active site depicting four glucosyl binding subsites. The nonreducing end glucosyl group is represented by G′ and the reducing end group by G. The catalytic site, designated by an arrow, is located between subsites −1 and 1.

(*21*, *23*−*26*) and quantified their individual contributions to transition-state stabilization during hydrolysis. In this study, the energetics of substrate−enzyme interactions were mapped in greater detail by analyzing 10 GA mutants located at four of the six highly conserved active site α → α loop regions with the series of deoxymaltose analogues.

In the first conserved α → α loop region of GA, several residues, including Tyr48, Trp52, Arg54, and Asp55, contribute to subsite −1 binding (*8*, *22*, *27*, *28*). Of these, the Asp55 → Gly mutation was chosen for this study since the side chain carboxyl group forms a bidentate hydrogen bond pattern with the 4′- and 6′-OH groups of the nonreducing end residue of an oligosaccharide inhibitor in subsite −1 (*7*, *9*, *13*). Previous kinetic analyses of Asp55 → Gly GA indicated that both these hydrogen bonds are most likely realized in the transition-state complex, but not in the ground-state complex (*28*).

Three mutants of highly conserved residues in the second α → α segment, Tyr116 → Ala (*29*), Ser119 → Tyr (*3*), and Trp120 → Phe (*15*), were previously shown to have different effects on activity. The most critical of these residues, Trp120, plays a crucial role in transition-state stabilization (*15*). Steady-state fluorescence studies indicated that Trp120 is substantially perturbed by substrate or inhibitor binding (*30*). In crystal structures of both free and complexed GA, a hydrogen bond exists between NE1 of Trp120 and OE2 of Glu179, the general acid catalyst (*7*, *9*, *13*). Steady-state (*15*, *29*) and pre-steady-state kinetic analyses (*31*, *32*) indicate that Trp120 is not involved in the hydrolytic step for maltose hydrolysis, but rather plays a major role in conformational changes to a productive complex (*31*) and product release (*31*).

The third conserved α → α region of GA contains the general acid catalyst, Glu179, and four mutants were investigated here, Asp176 → Asn, Trp178 → Arg, Glu180 → Gln, and Asn182 → Ala (*4*, *28*). Asp176 was previously suggested to be involved in transition-state stabilization but not in substrate binding (*4*). Trp178 is involved in substrate binding at subsite −1 via hydrophobic interactions and at subsite 1 via a hydrogen bond between the backbone carbonyl group and the 3-OH group of the glucosyl residue (*7*), consistent with the steady-state kinetic results obtained with the Trp178 → Arg mutation (*28*). Glu180 is critical for substrate binding in subsite 1 (*4*), forms a charged hydrogen bond with the 2-OH group of maltose as shown in molecular recognition studies (*21*, *24*) and supported by crystallography (*6*, *13*), and plays a role in the binding mechanism (*18*). Finally, Asn182 has a minor role in the bond-type specificity for the α-1,4- over the α-1,6-linkage (*28*).

Two mutants from the fifth GA α → α region, Tyr306 → Phe and Asp309 → Asn, were studied. In this region, the invariant Arg305 hydrogen bonds with the 2′- and 3-OH of maltose in subsites −1 and 1 as suggested by equivalent oligosaccharide inhibitor hydroxyl groups in GA crystal structures (*7*, *9*, *13*), while the neighboring Tyr306 has a small role in substrate binding (*28*). Asp309 forms a salt bridge with Arg305 and may thus indirectly affect binding at the 2′- and 3-OH groups (*7*, *9*, *13*). Mutation of Asp309 substantially altered both k_{cat} and K_M and, in particular, destabilized the isomaltose transition-state complex (*25*, *28*). While the interactions of Arg305 with the deoxygenated substrate analogues would have been very relevant to this investigation along with Tyr306 and Asp309, the available Arg305 → Lys mutant has extremely poor affinity for maltose (*28*), and would require prohibitive amounts of the substrate analogues. No mutations from either the fourth or sixth conserved regions were studied here.

The 10 single amino acid residues selected for the study presented here are in clearly different ways involved in GA substrate intereactions; some directly interact with substrate hydroxyl groups, some indirectly, and some apparently not at all. They, furthermore, have different effects on the various steps in the GA mechanism. Hydrogen bond interactions between proteins and sugar ligands have been identified previously using substrate analogues or mutant enzymes (*33*−*35*), and our study adds to these findings. The energetic contributions of the various hydrogen bond interactions also add to a growing set of data defining the contributions of charged and uncharged hydrogen bonds as originally outlined by Fersht (*36*). The energetic contributions of the various hydrogen bonds, however, can be complicated somewhat by the presence of bound water. If a hydrogen bond between a water molecule and a substrate or enzyme functional group is present in a particular substrate or protein configuration, but not in a substrate analogue or mutant protein configuration, the observed binding energies are masked by the energetic contribution of the displaced water molecule. These effects can only be identified when high-resolution crystal structures of both complexes are available.

MATERIALS AND METHODS

Enzyme and Substrate Preparation. Syntheses of the 1-deoxy- and 1,2-dideoxy-D-maltose, of 3-deoxy-, 6-deoxy-, 2′-deoxy-, 3′-deoxy-, and parent methyl β-D-maltoside (*23*), and of 4′- and 6′-deoxy-D-maltose (*24*) have been previously described. D-Maltose was obtained from Merck. Construction of expression plasmids and mutated genes, production, and purification of the wild type and Asp55 → Gly (*28*), Tyr116 → Ala (*29*), Ser119 → Tyr (*3*), Trp120 → Phe (*15*), Asp176 → Asn (*4*), Trp178 → Arg (*28*), Glu180 → Gln (*4*), Asn182 → Ala (*28*), Tyr306 → Phe, and Asp309 → Gly GAs (*28*) have been described previously. All GA variants studied here are of the full-length G1 form, and protein concentrations were determined spectrophotometrically at 280 nm using the following extinction coefficients: $\epsilon_m = 1.37 \times 10^5\ M^{-1}\ cm^{-1}$ for wild-type and most mutant GAs and $\epsilon_m = 1.30 \times 10^5\ M^{-1}\ cm^{-1}$ for the two tryptophan mutants (*37*).

Activity Measurements. All kinetic assays were performed at 45 °C in 0.05 M sodium acetate buffer (pH 4.5). Initial rates of glucose release were determined from aliquots removed at appropriate time intervals using glucose oxidase as described previously (*15*). In reactions with D-maltose and the methyl β-D-maltoside derivatives, only glucose was

Table 1: Kinetic Parameters for Hydrolysis of Maltose by Wild-Type and Mutant Glucoamylases at 45 °C and pH 4.5

enzyme	k_{cat} (s^{-1})	K_M (mM)	k_{cat}/K_M (mM^{-1} s^{-1})
wild-type[a]	9.2 ± 0.4	1.4 ± 0.2	6.4
Asp55 → Gly[a]	0.040 ± 0.001	1.5 ± 0.1	0.03
Tyr116 → Ala[b]	0.62 ± 0.02	0.57 ± 0.05	1.09
Ser119 → Tyr[c]	10.1 ± 0.4	1.10 ± 0.15	9.2
Trp120 → Phe[d]	0.178 ± 0.012	0.909 ± 0.147	0.195
Asp176 → Asn[e]	0.728 ± 0.029	6.22 ± 0.62	0.117
Trp178 → Arg[f]	1.86 ± 0.11	1.52 ± 0.28	1.22
Glu180 → Gln[e]	1.53 ± 0.05	41.4 ± 4.6	0.037
Asn182 → Ala[f]	11.6 ± 0.3	1.38 ± 0.01	8.4
Tyr306 → Phe[a]	8.2 ± 0.5	3.68 ± 0.67	2.23
Asp309 → Asn[a]	0.32 ± 0.2	5.0 ± 1.1	0.064

[a] From Ref (28). [b] From Ref (29). [c] From Ref (3). [d] From Ref (15); data taken at 50 °C. [e] From Ref (4); data taken at 50 °C. [f] From Ref (40); data taken at 50 °C.

detected in the hydrolysis products since methyl-β-D-glucose does not react with glucose oxidase under the assay conditions that were used (*21*, *24*). In reactions with 4′- or 6′-deoxy-D-maltose substrates, GA activity was determined relative to a standard containing equimolar amounts of D-glucose and either 4- or 6-deoxy-D-glucose, respectively (*24*).

The second-order rate constant, k_{cat}/K_M, was determined for at least two different concentrations of substrate varying by a factor of 2 or more to ensure that a linear dependence of activity on substrate concentration was fulfilled. Substrate concentrations were typically ≤0.1 mM for wild-type GA and mutant enzymes having K_M values similar to that of the wild type (approximately 1 mM), and ≤0.5 mM for mutant enzymes having higher K_M values. K_M values for substrate analogues are expected to be of a similar magnitude or higher as a potential binding group has been removed from the substrate. The individual kinetic parameters, k_{cat} and K_M, were not determined due to limited availability of the substrate analogues. Depending on the substrate analogue used and the activity of the mutant enzyme, typical enzyme concentrations varied from 0.24 to 10.8 μg/mL for wild-type GA and mutants with activity similar to that of the wild type (Ser119 → Tyr, Asn182 → Ala, and Tyr306 → Phe), and from 4.8 to 215 μg/mL for the remaining mutants with activity significantly lower than that of the wild type. Total reaction times ranged from 25 to 300 min. The error in k_{cat}/K_M determination was <10%.

RESULTS AND DISCUSSION

The interactions between GA functional residues and individual maltose hydroxyl groups were studied using a series of GA mutants and maltose analogues. On the basis of previously determined steady-state kinetic parameters (Table 1), the mutant enzymes investigated here should encompass a diverse set of GA active site interactions with the substrate maltose. Three mutants have k_{cat} values similar to that of the wild type, Ser119 → Tyr, Asn182 → Ala, and Tyr306 → Phe, while the remaining mutants have k_{cat} values from approximately 5- to 230-fold lower. Relative to that of the wild type, K_M values obtained for the mutant enzymes indicate that a substitution at Asp176, Glu180, Tyr306, or Asp309 increases K_M up to 30-fold, a substitution at Tyr116, Ser119, or Trp120 slightly decreases K_M, and substitutions at Asp55, Trp178, and Asn182 have no significant effect.

The change in transition-state stabilization caused by disrupting an interaction between the substrate and enzyme can be expressed quantitatively as $\Delta(\Delta G^{\ddagger}) = -RT \ln[(k_{cat}/K_M)_x/(k_{cat}/K_M)_y]$, where x represents either a mutant enzyme or a substrate analogue and y the wild-type enzyme or parent substrate (*36*, *38*). Via determination of the second-order rate constants, k_{cat}/K_M, for the various deoxymaltose analogues, the contribution of each of the hydroxyl groups to transition-state stabilization in maltose hydrolysis can be calculated. For wild-type GA, the 6′-, 4′-, 3′-, 3-, and 2-OH groups were previously shown in this way to provide 17.5, 18.8, 9.1, 11.3, and 5.2 kJ/mol, respectively, to transition-state stabilization (*21*, *24*). In those studies, the contributions of the three previously identified key polar groups for maltose hydrolysis, 6′-, 4′-, and 3-OH (*23*), were quantified along with the contributions of two other important groups, 3′- and 2-OH. The specific interaction between Glu180 and 2-OH of the reducing end glucose unit of maltose was kinetically identified using molecular recognition studies with the Glu180 → Gln GA mutant (*21*) and was later confirmed by several GA complex crystal structures (*5*−*7*, *9*, *13*). Here, such analysis of active site mutants with substate analogues is extended to include the eight hydroxyl groups of maltose and ten GA active site mutants. The second-order rate constants (k_{cat}/K_M) for hydrolysis of the maltose analogues with the different mutant and wild-type GAs were determined (Table 2), and the changes in free energy, $\Delta(\Delta G^{\ddagger})$, were calculated (Table 3). The mutants are in the highly conserved parts of α → α segments 1−3 and 5, representing four of the six $(\alpha/\alpha)_6$− loop regions forming the GA binding site. The locations of the mutated residues in the GA active site along with other key residues are shown in a stereodrawing depicting the GA active site−D-glucodihydroacarbose complex (Figure 2) (*9*, *13*).

Mutation in the First α → α *Segment.* Asp55 forms a bidentate hydrogen bond pattern with the glucosyl 4′- and 6′-OH groups at subsite −1 in the crystal structure of GA (*7*, *9*, *13*) (Figure 2). Because the mutation of Asp55 to Gly decreases k_{cat} more than 200-fold with no change in K_M compared to that of the wild type (*28*), Asp55 was concluded to be important during transition-state stabilization, but not in the Michaelis complex. The large difference in $\Delta(\Delta G^{\ddagger})$ values of more than 10 kJ/mol for this mutant compared to that of wild-type GA with both the 4′- and 6′-OH deoxy analogues (Table 3) clearly indicates that Asp55 interacts strongly with both these hydroxyl groups in transition-state stabilization. The Asp55 → Gly mutation also causes an approximately 5 kJ/mol decrease in $\Delta(\Delta G^{\ddagger})$ with each of the 3′-, 3-, and 6-OH groups (Table 3). The loss in binding contribution via the 4′- and 6′-OH groups caused by mutation at Asp55 apparently weakens the complex so that other substrate hydroxyl groups do not realize their full binding capacity in the GA transition-state complex. Removal of the acidic group may also influence other charged binding side chains contributing to destabilization of the complex.

Mutations in the Second α → α *Segment.* A striking feature of this mutational analysis of deoxymaltose analogues is that the free energy profiles of all three mutants in the Trp120 region, Tyr116 → Ala, Ser119 → Tyr, and Trp120 → Phe, are very similar to that of wild-type GA (Tables 2 and 3). These data agree with the crystal structures showing that none of these side chains bind to substrate OH groups. Despite

Table 2: Specificity Constants, k_{cat}/K_M (mM^{-1} s^{-1}), for Glucoamylase-Catalyzed Hydrolysis of a Series of Maltose Analogues at 45 °C and pH 4.5

enzyme	maltose	methyl β-D-maltoside	1-deoxy-maltose	1,2-dideoxy-maltose	methyl 3-deoxy-β-D-maltoside	methyl 6-deoxy-β-D-maltoside	methyl 2′-deoxy-β-D-maltoside	methyl 3′deoxy-D-maltoside	4′-deoxy-maltoside	6′-deoxy-maltoside
wild-type	7.3[a]	7.6[a]	13.8[a]	1.9[a]	0.11[a]	15.0[a]	6.8[b]	0.23[b]	5.9×10^{-3} [b]	1.0×10^{-2} [b]
Asp55 → Gly	2.4×10^{-2}	2.0×10^{-2}	0.28	7.9×10^{-3}	1.8×10^{-3}	0.35	2.5×10^{-2}	4.4×10^{-3}	2.3×10^{-3}	1.7×10^{-3}
Tyr116 → Ala	0.98	1.10	2.18	0.24	5.5×10^{-2}	2.11	1.9	0.14	3.3×10^{-3}	4.1×10^{-3}
Ser119 → Tyr	8.5	8.8	17.3	1.6	0.33	18.0	7.4	0.56	4.6×10^{-3}	9.5×10^{-3}
Trp120 → Phe	0.22	0.24	0.46	4.5×10^{-2}	3.4×10^{-3}	0.21	0.25	1.0×10^{-2}	2.1×10^{-4}	5.4×10^{-5}
Asp176 → Asn	9.6×10^{-2}	0.14	0.19	3.9×10^{-2}	4.1×10^{-3}	0.20	0.13	6.0×10^{-3}	9.3×10^{-5}	1.3×10^{-4}
Trp178 → Arg	1.1	0.90	1.1	0.23	3.3×10^{-2}	5.2	1.0	3.5×10^{-2}	0.16	0.19
Glu180 → Gln	2.1×10^{-2} [a]	6.6×10^{-3} [a]	1.7×10^{-2} [a]	2.2×10^{-2} [a]	9.4×10^{-5} [a]	2.3×10^{-2} [a]	4.2×10^{-2}	5.4×10^{-3}	9.4×10^{-4}	6.2×10^{-4}
Asn182 → Ala	4.9	3.6	4.2	0.41	0.23	9.6	4.6	0.50	8.8×10^{-3}	4.1×10^{-3}
Tyr306 → Phe	2.5	2.5	2.7	0.20	3.1×10^{-2}	0.18	4.7×10^{-2}	2.1×10^{-3}	1.9×10^{-3}	4.1×10^{-3}
Asp309 → Asn	7.4×10^{-2}	2.0×10^{-2}	0.28	7.9×10^{-3}	1.8×10^{-3}	0.35	2.5×10^{-2}	4.4×10^{-3}	2.3×10^{-3}	1.7×10^{-3}

[a] From ref *21*. [b] From ref *24*.

Table 3: Binding Energy Contribution $\Delta(\Delta G^{\ddagger})$ (kJ/mol) of Individual Substrate Hydroxyl Groups in the Hydrolysis of Maltose by Glucoamylase at 45 °C and pH 4.5[a]

enzyme	1-OH	2-OH	3-OH	6-OH	2′-OH	3′-OH	4′-OH	6′-OH
wild-type	−1.7	5.2	11.3	−1.8	0.2	9.1	18.8	17.5
Asp55 → Gly	−0.3	3.2	6.4	−7.5	−0.6	4.0	6.2	7.0
Tyr116 → Ala	−2.1	5.8	7.9	−1.8	−1.4	9.0	17.2	16.7
Ser119 → Tyr	−1.9	6.3	8.7	−1.9	0.4	7.3	19.4	17.5
Trp120 → Phe	−1.9	6.2	11.3	0.4	−0.1	8.3	18.4	21.9
Asp176 → Asn	−1.8	4.2	9.3	−1.0	0.2	8.3	18.4	17.4
Trp178 → Arg	−0.1	4.1	8.7	−4.6	−0.3	8.5	11.1	10.7
Glu180 → Gln	0.6	−0.7	11.2	−3.4	−0.6	4.8	8.3	9.4
Asn182 → Ala	0.9	6.2	7.3	−2.6	−0.6	7.9	16.7	18.7
Tyr306 → Phe	−0.3	6.5	11.5	−2.7	1.4	8.2	13.8	15.0
Asp309 → Asn	−1.6	7.9	7.9	−3.0	0.6	8.8	8.4	6.4

[a] $\Delta(\Delta G^{\ddagger}) = -RT \ln[(k_{cat}/K_M)_x/(k_{cat}/K_M)_y]$. For 1-OH, x is 1-deoxymaltose and y is maltose. For 2-OH, x is 1,2-dideoxymaltose and y is 1-deoxymaltose. For 3-OH, x is methyl 3-deoxy-β-D-maltoside and y is methyl β-D-maltoside. For 6-OH, x is methyl 6-deoxy-β-D-maltoside and y is methyl β-D-maltoside. For 2′-OH, x is methyl 2′deoxy-β-D-maltoside and y is methyl β-D-maltoside. For 3′-OH, x is methyl 3′-deoxy-β-D-maltoside and y is methyl β-D-maltoside. For 4′-OH, x is 4′-deoxymaltose and y is maltose. For 6′-OH, x is 6′-deoxymaltose and y is maltose.

changes in k_{cat} of more than 100-fold, and in K_M of ≤3-fold, the $\Delta(\Delta G^{\ddagger})$ values obtained with the mutant and wild-type GAs are very similar, with only a slight decrease in transition-state stabilization at the 3-OH group resulting from the Tyr116 and Ser119 mutations (Table 3). The Trp120 loop region has a critical role in catalysis, directing conformational changes found to accompany productive substrate binding and product release (*30*−*32*, *39*). The results obtained here indicate that any free energy changes required to induce this conformational change do not involve transition-state interactions with substrate hydroxyl groups.

Mutations in the Third α → α *Segment.* Each substitution of the four residues near the general acid catalyst Glu179 (Asp176, Trp178, Glu180, and Asn182) had a distinct influence on the steady-state parameters, suggesting different roles in activity. On the basis of the kinetic characterization of the Asp176 → Asn mutant GA, Asp176 was originally postulated to play a role in transition-state stabilization (*4*), although crystallographic structures indicate that Asp176 does not directly interact with the substrate (*6*, *7*, *9*, *13*). The $\Delta(\Delta G^{\ddagger})$ values obtained for the Asp176 → Asn mutation (Table 3) are essentially the same as for the wild type, in agreement with the lack of any direct hydrogen bonds with the substrate. Asp176, however, does hydrogen bond to both Glu179 and Glu180, which may explain the 4-fold increase in K_M and the 10-fold decrease in k_{cat} caused by the Asp176 → Asn mutation.

The indol ring of Trp178 contributes hydrophobic interactions with the substrate at subsite −1, and the backbone carbonyl group is hydrogen bonded with the substrate 3-OH in subsite 1 (*7*, *9*, *13*). The Trp178 → Arg mutation did not alter K_M, but k_{cat} decreased almost 10-fold (*28*). The $\Delta(\Delta G^{\ddagger})$ values obtained for the Trp178 → Arg mutant compared to that of wild-type GA (Table 3) indicate a contribution to transition-state stabilization of 3 kJ/mol by the 3-OH and also 6-OH, and 7−8 kJ/mol by the 4′- and 6′-OH group. This weakened transition-state stabilization for the 4′- and 6′-OH groups may reflect a loss in hydrophobic interactions in subsite −1, or the Arg substitution may result in a slightly different positioning of the Asp55 carboxylate which forms strong bidentate hydrogen bonds to the 4′- and 6′-OH groups in the crystal structures (*5*, *7*, *9*, *13*) as also indicated by the molecular recognition data (Table 3). The Trp178 → Arg substitution is expected to only modestly disturb the hydrogen bond between the 3-OH group and the backbone carbonyl group.

Glu180 has been shown both kinetically (*21*) and crystallographically (*6*, *9*, *13*) to hydrogen bond with the 2-OH group in subsite 1. In addition to this interaction, differences in the $\Delta(\Delta G^{\ddagger})$ values compared to that of wild-type GA of 4.3, 10.5, and 8.1 kJ/mol obtained for the 3′-, 4′-, and 6′-OH groups, respectively (Table 3), indicate important changes in subsite −1 as well as subsite 1. Similar perturbed protein−carbohydrate interactions at a neighboring subsite were previously demonstrated using isomaltose analogues as substrates for the Glu180 → Gln and Asp309 → Asn GA mutants (*25*). The Glu180 → Gln mutation removes a negatively charged side chain (*13*, *25*) which can either influence other side chains interacting through a hydrogen bond network or influence the pK_a of neighboring charged groups. An increase in the pK_a of Asp55 could decrease the strength of the hydrogen bonds to the substrate 4′- or 6′-OH groups.

The free energy profile obtained with Asn182 → Ala GA is very similar to that of the wild type, consistent with the same mutation showing no significant changes in the steady-state kinetic parameters for maltose hydrolysis (*28*). The 4 kJ/mol decrease in $\Delta(\Delta G^{\ddagger})$ with the 3-OH analogue (Table 3) at subsite 1 is likely the result of an indirect interaction as Asn182 in the GA crystal structure has no contacts with the substrate (*6*). Similarly, the Ser119 → Tyr GA shows a

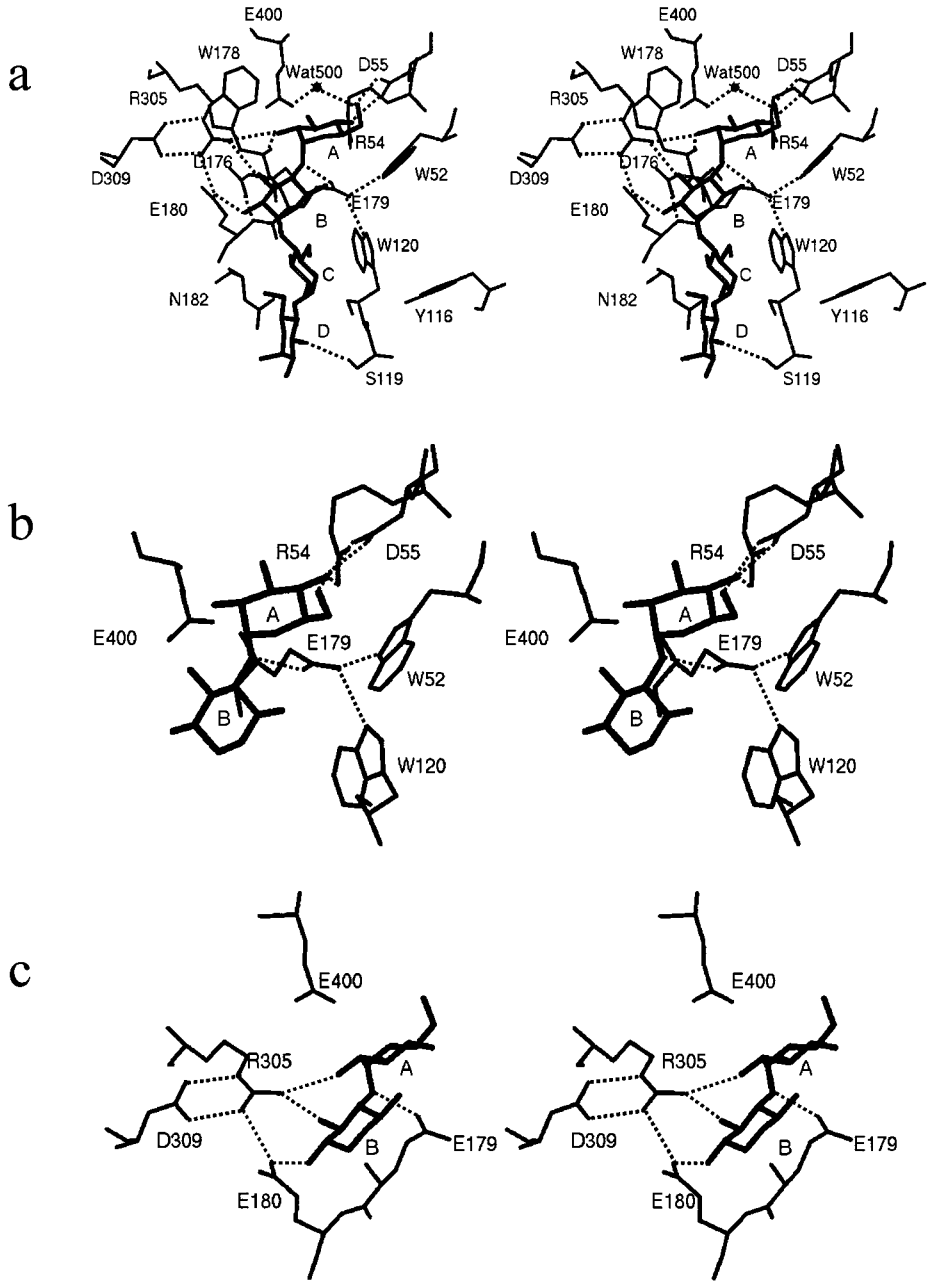

FIGURE 2: Stereoview of GA acarbose (rings A−D) interactions (*6*). (a) Highlight of the 10 positions where mutations were studied. In addition, Glu179 (the general acid catalyst), Glu400 (the base catalyst), Wat500 (water that remains in the complex and presumably plays the role of nucleophilic attack at C-1 in ring A of substrate), and Trp52, Arg54, and Arg305, all critical for activity and interacting with Glu179, 4-OH (ring A), 2-OH (ring A), and 3-OH (ring B), are included. (b) Closeup of one flank of the GA−acarbose binding site showing the Trp52, Arg54, Asp55, Trp120, and Glu179 interactions with the A and B units of acarbose. (c) Closeup showing the other flank with Glu179, Glu180, Arg305, and Asp309 interactions.

decrease in binding energy with the 3-OH group despite having steady-state parameters for maltose hydrolysis essentially unchanged from those of the wild type.

Mutations in the Fifth α → α *Segment.* The free energy profiles for mutations at Tyr306 and Asp309 from the fifth conserved region of GA are very different from each other (Table 3). The Tyr306 → Phe substitution only slightly decreased k_{cat} and increased K_M (*40*), and here, it is shown to weaken the binding energy contribution of the key polar 4′- and 6′-OH groups by 5 and 2.5 kJ/mol, respectively. The neighboring Arg305, however, hydrogen bonds with the 2′- and 3-OH based on oligosaccharide-based inhibitor structures (*7*, *9*, *13*). Removal of the 2′-OH group from maltose does not cause a significant change in the free energy with wild-type or Tyr306 → Phe GAs (Table 3), while removal of the 3-OH group increases $\Delta(\Delta G^{\ddagger})$ by 11 kJ/mol for both the mutant and wild-type GAs. These similar $\Delta(\Delta G^{\ddagger})$ values suggest that the hydrogen bond between Arg305 and the 3-OH is not disturbed by the replacement of Tyr306 by Phe.

Analysis of the hydrogen bond energetics between Arg305 and the 2′-OH requires additional explanation to account for expected electronic effects caused by the removal of the hydroxy group. 2-Deoxyglycosides have been shown to favorably stabilize the oxocarbenium ion-like transition state for glycoside hydrolysis, resulting in substantial rate accelerations (*41*−*44*). Despite these expected large rate accelerations, in this study removal of the 2′-OH group had virtually no influence on the $\Delta(\Delta G^{\ddagger})$ values (Table 3)

regardless of whether the individual GA mutations altered a charged or potentially charged active site side chain or not. There are at least two viable explanations for why the expected electronic effects of the 2-deoxyglycosides are not observed here. One explanation is that the large gain in transition-state stabilization from the electronic effects of the 2′-deoxy substitution is balanced by an equivalent loss in stabilization from the removed charged or uncharged hydrogen bond. Since substitution of the 2′-OH does not significantly impact the $\Delta(\Delta G^{\ddagger})$ values obtained for any of the 11 GA variants studied here, the expected increase in stabilization of the oxocarbenium ion transition state due to electronic effects must be offset by an equal but opposite destabilization of the complex due to the lost hydrogen bond or some other cause, in each mutation that was studied, no matter whether the mutation perturbs the charge distribution in the active site, binding interactions in the active site, or a residue distant from the active site. A second possible explanation for the lack of any observed rate enhancements of the 2-deoxyglycosides is that the electronic stabilization does occur, but it does not influence the transition-state complex. Previous reports have suggested that GA catalysis proceeds through an oxocarbenium ion-like transition state (*45*−*47*). These studies all utilized monosaccharide-based substrate derivatives of α-D-glucosyl fluoride. More recent studies have suggested that while bond hydrolysis may be the rate-limiting step for catalysis of monosaccharide-based substrates binding only to subsite −1, an alternative step other than bond hydrolysis is rate-limiting for GA-catalyzed hydrolysis of disaccharides and other substrates which occupy at least subsites −1 and 1 (*20*, *29*, *31*). On the basis of the proposed model from these studies, bond hydrolysis of the maltose and maltose analogues studied here would not be rate-limiting, and the electronic stabilization effect of the 2-deoxyglycosides on the oxocarbenium ion intermediate would therefore not be reflected in the observed k_{cat} values. The 2′-OH position according to this model simply does not have a significant effect on the observed nonhydrolytic rate-limiting step, accounting for the only minor changes observed in the $\Delta(\Delta G^{\ddagger})$ values. While either of these same two explanations can also be used to account for any observed electronic effects caused by deoxy substitutions of other hydroxyl groups, additional studies are required to address which best represents the actual catalytic mechanism for GA hydrolysis of maltose and other oligosaccharides.

The Asp309 → Asn mutation decreases k_{cat} 30-fold and increases K_M around 4-fold (*28*). Although not directly bound to substrate, Asp309 forms a salt bridge with Arg305 (*7*, *9*, *13*). Since the Asp309 mutation to Asn eliminates the salt bridge to Arg305, it can be expected to indirectly affect binding of Arg305 to the 2′- and 3-OH groups of maltose (Figure 2). From this work, however, the calculated energy contribution by the interaction with the 2′-OH group is minor and similar to that of wild-type GA (Table 3), and only a relatively small decrease in $\Delta(\Delta G^{\ddagger})$ of 3.4 kJ/mol is observed between the mutant and the 3-OH group, along with a 2.7 kJ/mol increase contributed by the 2-OH group (Table 3). Much more significant, however, are the decreases in binding energies of 10−11 kJ/mol realized with both the 4′- and 6′-OH groups resulting from the Asp309 → Asn mutation. These losses in binding energy at the two most critical subsite −1 interactions are similar to those calculated for the Glu180 → Gln and Trp178 → Arg substitutions. All three substitutions remove an acidic or introduce a basic side chain, and may influence the position and pK_a of Asp55 and thus its hydrogen bonds to the 4′- and 6′-OH groups. Arg54 which hydrogen bonds with the 4′-OH (Figure 2) may be influenced as well. The Asp309 → Asn mutation, which favors hydrolysis of the α-1,6- over the α-1,4-linkage compared to that of the wild type, had very similar effects on the subsite −1 free energy profile for both isomaltose (*25*) and maltose (Table 3) hydrolysis, supporting the notion that both these substrates adopt the same subsite −1 conformation. However, a clear difference between these two substrates is seen in subsite 1 where the 2-OH of maltose contributes 8 kJ/mol with the Asp309 mutant while the 2-OH of isomaltose makes only a negligible contribution. Such substrate-dependent effects support the validity of our approach of generating mutational analysis−substrate analogue energy profiles.

GA Mechanistic Implications. Quantification of the contribution of each of the various substrate hydroxyl groups toward transition-state stabilization in GA may be complicated by various factors. First, energetic contributions of hydrogen bonds between enzyme or substrate functional groups and water molecules have not been included. If a hydrogen bond with water exists in the parent enzyme or substrate, but not the mutant or deoxy analogue, the binding contribution of that functional group will be over- or underestimated. Of the residues studied here, on the basis of crystallographic structures (*5*, *6*), water molecules were found bound to Asp55, Trp120, and Glu180. A retained bound water would account for the rather low $\Delta(\Delta G^{\ddagger})$ values noticed between Glu180 and the 2-OH as noted earlier (*21*) and between Asp55 and the 4′- and 6′-OH groups. Second, substitution of enzyme or substrate functional groups may change the rate-limiting step for the reaction which may well happen given the substantial free energy changes resulting from several of the GA mutations as well as with some of the substrate analogues. The proposed minimal GA mechanism contains three steps, with the associated rate parameters:

$$E + G_x \underset{k_{-1}}{\overset{k_1}{\leftrightarrow}} EG_x \underset{k_{-2}}{\overset{k_2}{\leftrightarrow}} EX \overset{k_{cat}}{\leftrightarrow} E + P$$

where E represents the uncomplexed enzyme, G_x the substrate, EG_x an associated complex, EX either the enzyme product complex (*31*) or a second associated complex (*1*, *18*, *31*), and P the product. The rate-limiting step for maltose hydrolysis with GA (k_{cat} = 0.3 s^{-1} at 8 °C) occurs nearly 4000-fold more slowly than the first observable step (k_2 = 1392 s^{-1}) (*31*). A mutation, therefore, could hypothetically decrease k_2 nearly 4000-fold without changing either k_{cat} or K_M, and consequently cause no change in the free energy, $\Delta(\Delta G^{\ddagger})$, which depends only on the second-order rate constant, k_{cat}/K_M. For a mutation affecting only the second step to decrease transition-state stabilization, it will have to decrease the equivalent k_{cat}/K_M value for the second step (represented by k_2/K_1, where $K_1 = k_1/k_{-1}$) below the observed steady-state k_{cat}/K_M value. The difference in free energy between these two steps can be expressed with the equation $\Delta(\Delta G^{\ddagger}) = -RT \ln[(k_{cat}/K_M)_{G_x}/(k_2/K_1)_X]$, where G_x represents the kinetic parameters for the second step and X for the rate-limiting step. Using previously reported values for these rate constants at 8 °C (*31*), the difference in free energy between

these two steps is 10.5 kJ/mol. Therefore, for each mutation that decreases k_2 to such an extent that k_2 becomes the rate-limiting step instead of the step currently represented by k_{cat}, the change in transition-state stabilization resulting from that mutation would be underestimated by around 10 kJ/mol. This same analysis holds true if removing a substrate hydroxyl group changes the rate-limiting step from the step represented by k_{cat} to the step represented by k_2, and again, there may be a 10 kJ/mol underestimation of the contribution of that particular hydroxyl group to transition-state stabilization.

Pre-steady-state kinetic analysis can detect changes in the rates of E−S complex formation and the hydrolysis-associated step, and such analyses have already been performed on three of the mutant enzymes studied here, Trp120 → Phe, Asp176 → Asn, and Glu180 → Gln (*18*, *31*, *32*). For maltose hydrolysis at 8 °C, Trp120 → Phe GA decreased the steady-state kinetic parameters, k_{cat} and K_M, 30- and 3-fold, respectively, whereas there was no effect on the pre-steady-state rate constant, k_2, and only a small change in the association constant, K_1 (*31*, *32*, *39*). Trp120 thus plays only a very minor role in the first two observable steps represented by K_1, and k_2, but plays a major role in the rate-limiting step represented by k_{cat}. The results presented here indicate that mutation of Trp120 does not influence hydrogen bonding interactions with substrate OH groups, and the changes in k_{cat} and K_M resulting from mutation of Trp120 stem from other factors such as the conformational changes suggested in previous studies (*31*, *32*, *39*).

Substitution of Asp176, like the three mutations in the Trp120 region, did not result in any substantial changes in the free energy profiles of the substrate hydroxyl groups. Pre-steady-state kinetic analysis of the Asp176 → Asn enzyme (*18*) indicated a doubling of the initial dissociation rate constant, K_1, while the rate constant associated with the second step, k_2, was unchanged. Although Asp176 does not form hydrogen bonds with the substrate, it does play a major role in transition-state stabilization as evidenced by the 20-fold decrease in k_{cat} at 45 °C (*4*). Pre-steady-state analysis with wild-type GA has suggested that the predominant complexed enzyme form is the enzyme−product complex and not an enzyme−substrate complex (*31*). Therefore, the nearly 5-fold increase in K_M caused by the Asp176 mutation may be due to a decreased concentration of this enzyme−product complex. Conversely, the decreased K_M caused by all three mutations in the Trp120 region may then reflect an increased concentration of the enzyme−product complex.

Mechanistic Differences between Subsite −1 and Subsite +1 Interactions. Glu180 provides an interesting target for further probing the mechanistic and energetic differences between the various steps in the GA mechanism, in particular, for studying the energetics of the hydrolytic and product release steps since this residue hydrogen bonds with 2-OH, a bond which should be present in both the substrate and product complexes. At 8 °C, the Glu180 → Gln mutation compared to the wild type increases K_M more than 80-fold, but only decreases k_{cat} 2-fold, while the pre-steady-state kinetic parameter k_2 decreases 10-fold and the dissociation constant K_1 increases just 7-fold. Glu180 therefore decreases the rate of the fast step, k_2, 10-fold; however, this rate is still more than 600-fold faster than the rate of the slower step, k_{cat}, as measured in wild-type GA. These kinetic parameters suggest that removing the hydrogen bond with the 2-OH group of maltose does not change the rate-limiting step in the GA mechanism. The 7-fold increase in K_1 presumably reflects the decrease in the extent of formation of the initial maltose−enzyme complex due to removal of a hydrogen bond at subsite 1 (*27*). It is noteworthy that the Glu180 → Gln mutation increases the maltose dissociation constant, K_1, only 7-fold, but increases the total dissociation constant, K_M, 80-fold. Since substrate association is dominated by subsite −1 interactions (*18*, *20*), Glu180 plays a less important role in this step, influencing K_1 only moderately, whereas in the suggested enzyme−product complex (*30*), dominated by subsite 1, Glu180 plays a major role and strongly influences K_M.

On the basis of structural analysis (*7*, *9*, *13*), perturbation of hydrogen bond interactions between enzyme functional groups and the maltose 2′-, 3′-, 4′-, and 6′-OH groups is predicted to predominantly affect subsite −1 binding, with relatively little change to the binding of the reducing end product in subsite 1. These subsite −1 perturbations may influence more than substrate binding since they may also influence conformational changes associated with the transition state, and formation or dissociation of the product complex. Support for this argument is obtained from the steady-state kinetic parameters obtained with GA mutants at subsite −1 for maltose hydrolysis, i.e., Trp52 (*27*), Arg54 (*22*), Asp55 (*28*), and Trp178 (*40*), which all have K_M values similar to that of wild-type GA, despite very large changes in k_{cat}. Pre-steady-state analysis with the Trp52 → Phe mutant indicates no change in K_M or K_1, but a more than 600-fold decrease in k_{cat} (*27*). Mutation of Trp52 to Phe would not be expected to influence either K_M or K_1 since crystal structures do not indicate close contacts between inhibitors and Trp52, and the mutation maintains the aromatic nature of the side chain, and hence the possibility for hydrophobic interactions with the substrate. In contrast, mutation of Glu180 or Trp317, two residues influencing subsite 1, increases K_1 7-fold and K_M 27−80-fold, with much smaller effects on k_{cat} (*27*), indicating that subsite 1 interactions play an important though not dominant role in the initial substrate binding as reflected in K_1, but play a more important role in binding the additional complexes reflected in K_M.

General Trends. Some general trends can be noted in the free energy profiles of the various mutations. The 1-, 6-, and 2′-OH groups apparently contribute very little to transition-state stabilization, with removal of the 1- or 6-OH groups actually enhancing maltose hydrolysis in some cases (Table 2) (*21*, *24*). Removal of hydrogen bonds to either the 2- or 3-OH of the reducing end glucose substantially decreases the turnover rate for maltose hydrolysis, k_{cat}, as evidenced by Glu180 → Gln GA, in which a hydrogen bond to the 2-OH group is removed. Since a conformational change is likely involved in the rate-limiting step, the 2-OH and probably 3-OH groups have critical roles in this process.

Removal of the 6-OH group increases k_{cat}/K_M even with the wild type; however, substantially larger increases occurred for Asp55 → Gly, Trp178 → Arg, Glu180 → Gln, and Asp309 → Asn GAs. All four of these mutations diminish the negative charge in the active site and cause a large decrease in the energetic contributions of the 4′- and 6′-OH groups. The effect is particularly noticeable in Asp55 → Gly GA, where removal of the 6-OH group increases transition-state stabilization nearly 6 kJ/mol more than in

the wild type. A possible explanation for the faster rates for these mutants with the 6-deoxy substrate is that the decreased level of binding in the mutants at the 4′- and 6′-OH groups in subsite −1 results in a complex which is also bound less tightly at the 6-OH in subsite 1 and subsequent removal of the 6-OH group reduces steric interference in the transition-state complex. Tight binding at the 4′- and 6′-OH groups of subsite −1 would then be a prerequisite for the enzyme to favorably interact at subsite 1.

Conclusions. The combination of molecular recognition using substrate analogues and site-directed mutagenesis has successfully been used previously to identify and quantify interactions between various functional groups in GA and maltose or isomaltose (*21*, *24*, *25*). Here, we extend such an analysis by studying a series of maltose analogues and a set of 10 GA mutant enzymes. Mutation of residues not hydrogen bonding directly to substrate as seen in the crystal structure, i.e., Tyr116, Ser119, Trp120, and Asp176, has little or no effect on the free energy profiles representing the binding energy contributions of each of the maltose hydroxyl groups. The energetics of two GA side chains shown to form hydrogen bonds with maltose on the basis of crystallographic evidence of pseudotetrasaccharide GA complexes (*7*, *9*, *13*), Glu180−2-OH and Asp55−4′-OH and −6′-OH, can be quantitatively defined. In those enzyme variants where the ionization properties at the active site were potentially altered, i.e., the mutations of Asp55, Trp178, Glu180, and Asp309, multiple perturbations with hydroxyl groups at subsites −1 and 1 were observed. The change in pK_a values resulting from the change in local charge, particularly of the important Asp55 side chain, may account for these perturbations. While the strongest bond energies are always measured in subsite −1, these interactions are critical for substrate binding and bond hydrolysis, but should not contribute to the reducing end product release step.

ACKNOWLEDGMENT

We thank Klaus Bock and Susanne Refn for the generous gift of the various substrate analogues and Jørgen Sauer for help with Figure 2.

REFERENCES

1. Hiromi, K., Ohnishi, M., and Tanaka, A. (1983) *Mol. Cell. Biochem. 51*, 79−95.
2. Hiromi, K., Kawai, M., and Ono, S. (1966) *J. Biochem. 59*, 476−480.
3. Sierks, M. R., and Svensson, B. (1994) *Protein Eng. 7*, 1479−1484.
4. Sierks, M. R., Ford, C., Reilly, P. J., and Svensson, B. (1990) *Protein Eng. 3*, 193−198.
5. Harris, E. M. S., Aleshin, A. E., Firsov, L. M., and Honzatko, R. B. (1993) *Biochemistry 32*, 1618−1626.
6. Aleshin, A. E., Firsov, L. M., and Honzatko, R. B. (1994) *J. Biol. Chem. 269*, 15631−15639.
7. Aleshin, A. E., Hoffman, C., Firsov, L. M., and Honzatko, R. B. (1994) *J. Mol. Biol. 238*, 575−591.
8. Frandsen, T. P., Dupont, C., Lehmbeck, J., Stoffer, B., Sierks, M. R., Honzatko, R., and Svensson, B. (1994) *Biochemistry 33*, 13808−13816.
9. Aleshin, A. E., Stoffer, B., Firsov, L. M., Svensson, B., and Honzatko, R. B. (1996) *Biochemistry 35*, 8319−8328.
10. Itoh, T., Ohtsuki, I., Yamashita, I., and Fukui, S. (1987) *J. Bacteriol. 169*, 4171−4176.
11. Coutinho, P. M., and Reilly, P. J. (1994) *Protein Eng. 7*, 749−760.
12. Henrissat, B., Coutinho, P. M., and Reilly, P. J. (1994) *Protein Eng. 7*, 1281−1286.
13. Stoffer, B., Aleshin, A. E., Firsov, L. J., Svensson, B., and Honzatko, R. B. (1995) *FEBS Lett. 358*, 57−61.
14. Meagher, M. M., Nikolov, Z. L., and Reilly, P. J. (1989) *Biotechnol. Bioeng. 34*, 681−688.
15. Sierks, M. R., Ford, C., Reilly, P. J., and Svensson, B. (1989) *Protein Eng. 2*, 621−625.
16. Hiromi, K. (1970) *Biochim. Biophys. Acta 40*, 1−6.
17. Fagerstrom, R. (1991) *J. Gen. Microbiol. 137*, 1001−1008.
18. Christensen, U., Olsen, K., Stoffer, B. B., and Svensson, B. (1996) *Biochemistry 35*, 15009−15018.
19. Ohnishi, M. (1990) *Staerke 42*, 311−313.
20. Natarajan, S., and Sierks, M. R. (1997) *Biochemistry 36*, 14946−14955.
21. Sierks, M. R., and Svensson, B. (1992) *Protein Eng. 5*, 185−188.
22. Frandsen, T. P., Christensen, T., Stoffer, B., Lehmbeck, J., Dupont, C., Honzatko, R. B., and Svensson, B. (1995) *Biochemistry 34*, 10162−10169.
23. Bock, K., and Pedersen, H. (1987) *Acta Chem. Scand. B42*, 617−628.
24. Sierks, M. R., Bock, K., Refn, S., and Svensson, B. (1992) *Biochemistry 31*, 8972−8977.
25. Frandsen, T. P., Stoffer, B. B., Palcic, M. M., Hof, S., and Svensson, B. (1996) *J. Mol. Biol. 263*, 79−89.
26. Lemieux, R. U., Spohr, U., Bach, M., Cameron, D. R., Frandsen, T. P., Stoffer, B. B., Svensson, B., and Palcic, M. M. (1996) *Can. J. Chem. 74*, 319−335.
27. Christensen, T., Stoffer, B., Svensson, B., and Christensen, U. (1997) *Eur. J. Biochem. 250*, 638−645.
28. Sierks, M. R., and Svensson, B. (1993) *Biochemistry 32*, 1113−1117.
29. Sierks, M. R., and Svensson, B. (1996) *Biochemistry 35*, 1865−1871.
30. Svensson, B., and Sierks, M. (1992) *Carbohydr. Res. 227*, 29−44.
31. Natarajan, S., and Sierks, M. R. (1996) *Biochemistry 35*, 15269−15279.
32. Olsen, K., Christiansen, U., Sierks, M. R., and Svensson, B. (1993) *Biochemistry 32*, 9686−9693.
33. Mikrad, R. V., Beierbeck, H., and Lemieux, R. U. (1992) *Am. J. Chem. 30*, 241−253.
34. McCarter, J. D., Adams, J. F., and Withers, S. G. (1992) *Biochem. J. 286*, 721−727.
35. Hindsgaul, O., Khare, D. P., Bach, M., and Lemieux, R. U. (1985) *Can. J. Chem. 63*, 2653−2658.
36. Wilkinson, A. J., Fersht, A. R., Blow, D. M., and Winter, G. (1983) *Biochemistry 22*, 3581−3586.
37. Clarke, A. J., and Svensson, B. (1984) *Carlsberg Res. Commun. 49*, 111−122.
38. Street, I. P., Armstrong, C. R., and Withers, S. G. (1986) *Biochemistry 25*, 6021−6027.
39. Natarajan, S., and Sierks, M. R. (1996) *Biochemistry 35*, 3050−3058.
40. Sierks, M. R., Ford, C., Reilly, P. J., and Svensson, B. (1993) *Protein Eng. 6*, 75−79.
41. Namchuk, M. N., and Withers, S. G. (1995) *Biochemistry 34*, 16194−16202.
42. Ly, H. D., and Withers, S. G. (1999) *Annu. Rev. Biochem. 68*, 487−522.
43. Davies, G., Sinnott, M. L., and Withers, S. G. (1998) in *Comprehensive Biological Catalysis* (Sinnott, M., Ed.) pp 119−208, Academic Press, San Diego, CA.
44. Calugaru, S., Krishan, S., Chany, C. J., Hall, B. G., and Sinnott, M. L. (1997) *Biochem. J. 325*, 117−121.
45. Tanaka, Y., Tao, W., Blanchard, J. S., and Hehre, E. J. (1994) *J. Biol. Chem. 269*, 32306−32312.
46. Konstantinidis, A., and Sinnott, M. L. (1991) *J. Biochem. 279*, 587−593.
47. Matsui, I., Ishikawa, K., Miyairi, S., Fukui, S., and Honda, K. (1991) *Biochim. Biophys. Acta. 1077*, 416−419.

BI9925219